

## Synchronization-based image edge detection

G. W. WEI<sup>1,2</sup> and Y. Q. JIA<sup>1</sup>

<sup>1</sup> *Department of Computational Science, National University of Singapore  
Singapore 117543, Singapore*

<sup>2</sup> *Department of Mathematics, Michigan State University  
East Lansing, MI 48824, USA*

(received 14 January 2002; accepted in final form 20 June 2002)

PACS. 05.45.Xt – Synchronization; coupled oscillators.

PACS. 05.45.-a – Nonlinear dynamics and nonlinear dynamical systems.

PACS. 07.05.Pj – Image processing.

**Abstract.** – This letter proposes a novel image edge detection algorithm based on the difference of two synchronizing spatially extended nonlinear dynamical systems. The time evolution of each system is identified as a low-pass filtering process, whereas the difference of two synchronizing states is identified as the result of high-pass filtering. Two systems are weakly coupled and allowed to take a common image as their initial value, but have different time scales in their dynamical motions. Results are compared with those of standard image processing schemes. Some of the best image edges could be obtained by an appropriate balance between synchronization and desynchronization.

There has been a great deal of interest in the synchronization phenomenon in the recent years [1–12]. The modern theory of synchronization is rich in its content due to rapid developments in theoretical and computational analyses and a broad spectrum of applications. Synchronization is of fundamental importance in secure communication [2], electronic circuits [3], nonlinear optics [4], chemical and biological systems [5]. More recently, the study of synchronization has led to an efficient control of wake turbulence and a robust shock-capturing scheme which provides an effective technique for the understanding of hyperbolic conservation laws [6]. Synchronization-associated signal processing and pattern recognition have been discussed [7]. Some of the most important synchronizations include lag synchronization [8], phase synchronization [9], generalized synchronization [10], and complete synchronization [11]. Among them, complete synchronization has the strongest correlation between two interacting systems. Most recently, the relationship and definition of various synchronizations have been discussed [12]. It is well known that, in many cases, synchronization is not ideal. For example, the similarity function of the lag synchronization has rarely been found to be identical to zero [8]. The residual of synchronization, defined by the difference of two synchronizing states, is generally considered as an undesirable aspect. Thus, the utility of synchronization residual has not been addressed, to our knowledge. In particular, the image filter property of a synchronization process is not well understood.

A key issue in pattern recognition, computer vision, target tracking and image processing is the detection of image edges. The latter usually refers to rapid changes in some physical properties, such as geometry, illumination, and reflectivity. The edge detection process serves

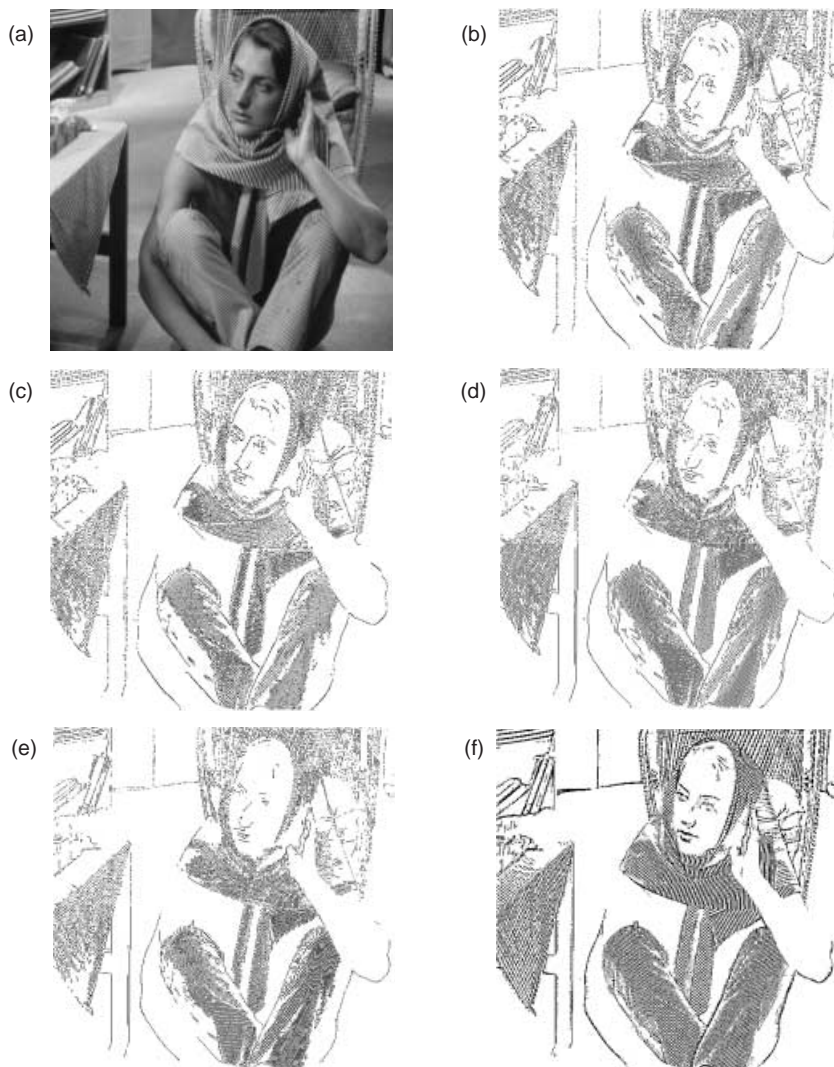


Fig. 1 – (a) The original Barbara image; (b) edges detected by the Sobel detector; (c) edges detected by the Prewitt detector; (d) edges detected by the Canny detector; (e) edges detected by the anisotropic diffusion scheme; (f) edges detected by the synchronization scheme.

to simplify the analysis of image by dramatically reducing the amount of data to be processed, meanwhile preserving useful structural information about the object [13]. Standard edge detectors, such as the Sobel and Prewitt detectors, are finite-difference-based first-derivative operators, which pick up high-frequency responses at image edges. Recently, Canny [14] has formulated edge detection as an optimization problem, and the Canny detector can be effectively approximated by the first derivative of the Gaussian function. Despite the great success of traditional image processing techniques, the problem of quality edge detection with many real-world images remains unsolved due to large amount of textures. Solution of this problem is of pressing importance to both practical and scientific interest, such as missile guiding and biomedical imaging. Figure 1(a) depicts a standard test image, the Barbara

image which is of 8 bits in resolution and has  $512 \times 512$  pixels in size. The Barbara image contains much high-frequency texture and is a severe test case for most existing edge detection methods. We employ the standard Sobel, Prewitt and Canny detectors [14] to extract edges of the Barbara image. Figures 1(b), (c) and (d) show the image edges obtained by using these detectors with a standard threshold technique [15]. It is seen that none of these detectors gives correct edge response to the texture part of the Barbara image. The regularity of the thin lines in the original image has been entirely distorted. The purpose of this letter is to introduce a synchronization-based realistic edge detection scheme for image edge detection and pattern recognition.

We consider two coupled dynamical systems given by

$$u_t = F_1(u, \nabla u, \nabla^2 u, \dots) + \varepsilon_1(v - u), \quad (1)$$

$$v_t = F_2(v, \nabla v, \nabla^2 v, \dots) + \varepsilon_2(u - v), \quad (2)$$

where  $u(x, y, t)$  and  $v(x, y, t)$  are scalar fields on a domain  $\Omega$  of interest and  $\varepsilon_1, \varepsilon_2$  are the coupling strengths. Here,  $F_1$  and  $F_2$  are nonlinear functions. To arrive at an algorithm for image processing, we consider a generalized flux vector

$$\mathbf{j}_1(x, y, t) = -d_1(|\nabla u|)\nabla u(x, y, t), \quad (3)$$

where  $d_1(|\nabla u|)$  is a function of local gradient which controls the mobility. In this work, the mobility function is chosen as a non-increasing function of the gradient, *e.g.*, a Gaussian

$$d_1(|\nabla u|) = \Gamma_1 \exp \left[ -\frac{|\nabla u|^2}{2\sigma_1^2} \right], \quad (4)$$

where  $\Gamma_1$  is positive semi-definite. Here  $\sigma_1^2$  is the variance defined by

$$\sigma_1^2(t) = \frac{1}{NM} \sum_{i=1}^N \sum_{j=1}^M [u(x_i, y_j, t) - \bar{u}(x_i, y_j, t)]^2, \quad (5)$$

where  $\bar{u}$  is the mean of  $u$  and  $N$  and  $M$  are the data length in the  $x$  and  $y$  directions, respectively. The conservation requires

$$F_1 = -\nabla \cdot \mathbf{j}_1(x, y, t) = \nabla \cdot [d_1(|\nabla u|)\nabla u]. \quad (6)$$

Equation (6) can be recognized as an anisotropic diffusion operator [16] and has been used for image noise removal provided that  $u(x, y, 0) = I(x, y)$  is an image. The anisotropic diffusion can be used to describe the boundary-restricted diffusion, multiphase chemical reaction and reaction-diffusion in porous media. It was generalized [17] to include hyper-flux vectors which, in physics, describe a number of complex phenomena, such as pattern formation in alloys, glasses, polymers, combustion and biological systems.

The essential idea behind eq. (6) for image processing is as follows. The evolution of an image surface under a partial differential operator can be viewed as a form of image processing. Interestingly, the reverse is also true, *i.e.*, an image-processing method corresponds to the action of a partial differential equation (PDE), with suitable restrictions. Similar to the coupling scheme used in synchronizing conventional oscillators, the anisotropic diffusion equation is capable of removing certain oscillations on an image surface and produces a smoothed copy of the original image. Equation (6) provides a potential algorithm for image edge detection, segmentation, noise removal, and enhancement [17]. In this work, we use eq. (6) to extract

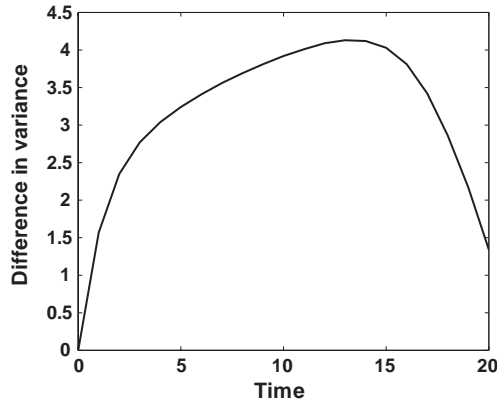


Fig. 2 – Difference in variance *vs.* time.

edges of the Barbara image. The fourth-order Runge-Kutta (RK4) scheme is used for the temporal discretization and a discrete singular convolution (DSC) algorithm is utilized for the spatial discretization. The DSC is a local spectral method and its use in scientific and engineering computations has been extensively validated [18]. Results of eq. (6) for the Barbara image are plotted in fig. 1(e), obtained using the anisotropic diffusion operator with the standard threshold technique [15]. Obviously, the anisotropic diffusion operator also seriously distorts image textures and the result is similar to those in figs. 1(b)-(d).

Despite restricted diffusion at image edges, the anisotropic diffusion is inherently a smoothing operation. Therefore, the high-frequency texture of an image is easily distorted during the smoothing. From the point of view of image processing, a smoothing operation is a low-pass filter. Whereas, image detection should be a high-pass filtering process. Therefore, the difference operators, such as the Sobel and Prewitt ones, are frequently used in the field. This analysis motivates us to speculate that the difference (residual) in the synchronization of two dynamical systems,

$$r(x, y, t) = u(x, y, t) - v(x, y, t), \quad (7)$$

might correspond to image edges as if obtained by high-pass filters, provided that their initial value is a common digital image field  $u(x, y, 0) = v(x, y, 0) = I(x, y)$ . In the rest of this letter, we explore the use of synchronization residual,  $r(x, y, t)$ , for image edge detection. It is believed that this study is of importance to the development of synchronization-based security and information processing algorithms.

The task of image processing is quite different from ordinary chaos synchronization and control. On the one hand, there should be much synchronized features in the dynamics in order for their residual to be physically meaningful. On the other hand, there should be substantial desynchronized features so that the residual could carry a sufficient amount of physical information. Thus, a practical and superior scheme for image processing would require a cutting edge balance between synchronization and desynchronization. Such a balance is determined by the selection of  $F_1$  and  $F_2$ , and of time in eq. (7). To ensure sufficient synchronized features, we limit ourselves to the case where both  $F_1$  and  $F_2$  have the same form of the mobility function as given by the anisotropic diffusion operator, eq. (6). Moreover, a common initial value, *i.e.*, the digital image  $I(x, y)$ , is chosen for both  $u(x, y, 0)$  and  $v(x, y, 0)$ . Therefore, there is an initial synchronized ( $r \sim 0$ ) period. However, to attain an appropriate image edge contrast, two dynamical systems must differ dramatically in their time scales of

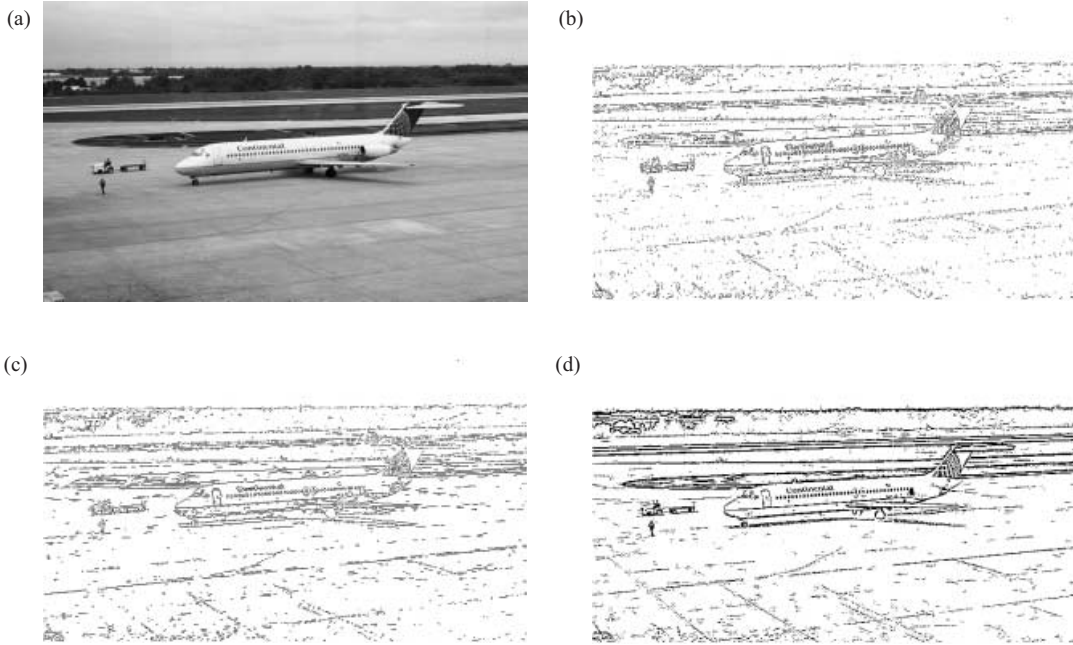


Fig. 3 – (a) The original aircraft image; (b) edges detected by the Canny detector; (c) edges detected by the anisotropic diffusion scheme; (d) edges detected by the synchronization scheme.

motion. This can be realized by setting  $\Gamma_1 \gg \Gamma_2$  and meanwhile setting both  $\varepsilon_1$  and  $\varepsilon_2$  to be relatively small so that the rate of change of  $u$  is dominated by the diffusion. As both systems are parabolic in nature, they will synchronize at a sufficiently long time, *i.e.*, they converge to each other in the norm

$$\lim_{t \rightarrow \infty} \|u(x, y, t) - v(x, y, t)\| = 0, \quad (8)$$

for a common initial value  $I(x, y)$  and appropriate parameters  $\Gamma_q$  and  $\varepsilon_q$  ( $q = 1, 2$ ). For image processing, we are interested in the *non-zero* synchronization residual at a *finite* time. Figure 2 plots the difference in variance  $[\sigma_2^2(t) - \sigma_1^2(t)]$  of two dynamical systems against the evolution time. It is found that best results are obtained when such a difference approaches its maximum.

Figure 1(f) depicts edges of the Barbara image detected by the synchronization residual  $r(x, y, t)$  at  $t = 11$ , with the same threshold technique [15] as used in all earlier cases. The parameters  $\Gamma_1 = 0.15$ ,  $\Gamma_2 = 0.01\Gamma_1$  and  $\varepsilon_1 = \varepsilon_2 = 0.01\Gamma_1$  are used in our computation. In fact, a wide range of parameters that satisfy  $\Gamma_1 \gg \Gamma_2, \varepsilon_1, \varepsilon_2$  would deliver similar results. The DSC and RK4 schemes are utilized for spatial and temporal discretizations, respectively. Obviously, facial edges are accurately extracted by the proposed approach. Moreover, the image texture is also clearly detected without distortion. To our knowledge, the image edges given by the synchronization residual are some of the best ever obtained for this severe case.

It remains to be verified that the proposed approach is robust and general for image edge detection. To this end, we test the proposed scheme on an aircraft image (8 bits resolution and  $659 \times 409$  pixels in size [15]) as shown in fig. 3(a). The ability of resolving some details, such as the characters “Continental”, could be crucial to pattern recognition and target tracking. This is a challenge to most existing edge detection algorithms. In this study, we employ the

standard Canny detector and the anisotropic diffusion operator for a comparison and their optimal results are given in figs. 3(b) and (c), respectively. As shown in fig. 3(d), the edges detected by synchronization residual are much superior to those of the other two schemes. The characters “Continental” are clearly resolved by the proposed approach.

In conclusion, a synchronization-based realistic scheme is proposed for image processing with an emphasis on image edge detection. Two weakly coupled, spatially extended nonlinear parabolic systems are identified as image low-pass filters and their difference is identified as an image high-pass filter. To construct a practical and efficient image-processing scheme, a balance between synchronization and desynchronization is sought. Two systems are allowed to take a common initial value, a digital image, but to evolve at two sharply different time scales so that their synchronization residual is significantly large for a finite time period. The synchronization residual is utilized for edge detection of texture images, which are difficult for existing approaches. Some of the best results are obtained by using the proposed approach for two standard test images, the Barbara and the aircraft.

## REFERENCES

- [1] OTT E., GREBOGI C. and YORKE J. A., *Phys. Rev. Lett.*, **64** (1990) 1196.
- [2] KOCAREV L. and PARLITZ U., *Phys. Rev. Lett.*, **74** (1995) 5028; LAI C. H., ZHOU C. T. and YU M. Y., *Phys. Scr.*, **59** (1999) 198.
- [3] ANISHCHENKO V. C., VADIVASOVA T. E., ASTAKHOV V. V., SOSNOVTSEVA O. V., WU C. W. and CHUA L. O., *Int. J. Bifurcation Chaos*, **5** (1995) 1677; HEAGY J. F., CARROLL T. L. and PECORA L. M., *Phys. Rev. A*, **50** (1994) 1874.
- [4] FABINY L., COLET P. and ROY R., *Phys. Rev. A*, **47** (1993) 4287; ROY R. and THORNBURG K. S. jr., *Phys. Rev. Lett.*, **72** (1994) 2009.
- [5] SCHREIBER I. and MAREK M., *Physica (Amsterdam) D*, **5** (1982) 258; HAN S. K., KURRER C. and KURAMOTO Y., *Phys. Rev. Lett.*, **75** (1995) 3190.
- [6] WEI G. W., *Phys. Rev. Lett.*, **86** (2001) 3542; PATNAIK B. S. V. and WEI G. W., *Phys. Rev. Lett.*, **88** (2002) 054502.
- [7] LINDNER J. F., MEADOWS B. K., DITTO W. L., INCHIOSA M. E. and BULSARA A. R., *Phys. Rev. Lett.*, **75** (1995) 3.
- [8] ROSENBLUM M. G., PIKOVSKY A. S. and KURTHS J., *Phys. Rev. Lett.*, **78** (1997) 4193; ZHAN M., WEI G. W. and LAI C. H., *Phys. Rev. E*, **65** (2002) 036202; TAHERION S. and LAI Y. C., *Phys. Rev. E*, **59** (1999) R6247.
- [9] ROSENBLUM M. G., PIKOVSKY A. S. and KURTHS J., *Phys. Rev. Lett.*, **76** (1996) 1804; YALCINKAYA T. and LAI Y. C., *Phys. Rev. Lett.*, **79** (1997) 3885; LIU Z., LAI Y. C. and HOPPENSTEADT F. C., *Phys. Rev. E*, **63** (2001) 055201.
- [10] RULKOV N. F., SUSHCHIK M. M., TSIMRING L. S. and ABARBANEL H. D. I., *Phys. Rev. E*, **51** (1995) 980; KOCAREV L. and PARLITZ U., *Phys. Rev. Lett.*, **76** (1996) 1816.
- [11] PECORA L. M. and CARROLL T. L., *Phys. Rev. Lett.*, **64** (1990) 821; ZHAN M., HU G. and YANG J., *Phys. Rev. E*, **62** (2000) 2963.
- [12] BROWN R. and KOCAREV L., *Chaos*, **10** (2000) 344; BOCCALETTI S., PECORA L. M. and PELAEZ A., *Phys. Rev. E*, **63** (2001) 066219.
- [13] HOU Z. J. and WEI G. W., *Pattern Recognit.*, **35** (2002) 1559.
- [14] CANNY J., *IEEE Trans. Pattern Anal. Machine Intell.*, **8** (1986) 679.
- [15] HEATH M., SARKAR S., SANOCKI T. and BOWYER K. W., *IEEE Trans. Pattern Anal. Machine Intell.*, **19** (1997) 1338.
- [16] PERONA P. and MALIK J., *IEEE Trans. Pattern Anal. Machine Intell.*, **12** (1990) 629.
- [17] WEI G. W., *IEEE Signal Proc. Lett.*, **6** (1999) 165.
- [18] WEI G. W., *J. Chem. Phys.*, **110** (1999) 8930; *Physica D*, **137** (2000) 247; *Comput. Methods Appl. Mech. Engng.*, **190** (2001) 2017; *J. Sound Vibrat.*, **244** (2001) 535.